Positional Isotope Exchange and Kinetic Experiments with *Escherichia coli* Guanosine-5′-monophosphate Synthetase[†]

Wolfgang von der Saal, Carl S. Crysler, and Joseph J. Villafranca*

Department of Chemistry, The Pennsylvania State University, University Park, Pennsylvania 16802

Received February 19, 1985

ABSTRACT: The kinetic mechanism of *Escherichia coli* guanosine-5′-monophosphate synthetase has been determined by utilizing initial velocity kinetic patterns and positional isotope exchange experiments. The initial velocity patterns of MgATP, XMP, and either NH_3 or glutamine (as nitrogen source) were consistent with the ordered addition of MgATP followed by XMP and then NH_3. The enzyme catalyzes the exchange of ^{18}O from the β-nonbridge positions of $[β,β,βγ,γ,γ,γ-^{18}O_6]ATP$ into the αβ-bridge position only in the presence of XMP and Mg^{2+}. The exchange reaction did not require NH_3. The isotope exchange reaction increased as the XMP concentration increased and then decreased at saturating levels of XMP. These results also support the ordered addition of MgATP followed by XMP. GMP synthetase catalyzes the hydrolysis of ATP to AMP and PP_i along with an ATP/PP_i exchange reaction in the absence of NH_3. These data taken together support a mechanism in which the initial step in the enzymatic reaction involves formation of an adenyl-XMP intermediate. Psicofuranine, an irreversible inhibitor of the enzyme, acts by preventing the release or further reaction of adenyl-XMP with H_2O or NH_3 but does not suppress the isotope exchange or ATP/PP_i exchange reactions. GMP synthetase has also been shown to require a free divalent cation for full activity. When Ca^{2+} replaces Mg^{2+} in the reaction, the positional isotope exchange reaction is enhanced but the reaction with NH_3 to form GMP is greatly suppressed.

GMP synthetase [xanthosine-5′-phosphate:ammonia ligase (AMP-forming), EC 6.3.4.1] from *Escherichia coli* B 96 has a molecular weight of approximately 126 000 and consists of two subunits. It catalyzes the reaction

$$XMP + ATP + NH_3 \xrightarrow{Mg^{2+}} GMP + AMP + PP_i \quad (1)$$
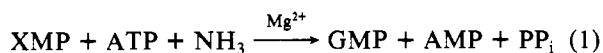
In preliminary investigations of the enzyme mechanism, transfer of ^{18}O from the 2-hydroxy group of XMP (**1**) was detected (Lagerkvist, 1958; Abrams & Bentley, 1959) as well as chromatographic evidence for the formation of an adenyl-XMP intermediate (**3**) (Fukuyama, 1966). However, no ATP/PP_i exchange could be detected in the absence of ammonia, which may due to the fact that PP_i is released from the enzyme only after the addition of ammonia or that PP_i is not released from the enzyme in the partial reaction. To provide evidence for a stepwise mechanism for this reaction, the positional isotope exchange (PIX)[1] method (Midelfort & Rose, 1976) was used because it is independent of the exchange of PP_i between the enzyme and solution (DeBrosse & Villafranca, 1983) (Scheme I). This method is also ideal for evaluating the relative rates of formation of intermediates in enzyme-catalyzed reactions. Since the steady-state mechanism for this enzyme has not been determined, we decided to investigate the kinetics of the forward reaction. These experiments combined with PIX experiments can provide evidence for the random or ordered addition of the substrates (Scheme II). The use of PIX experiments for this purpose has recently been described by Raushel & Garrard (1984).

The stoichiometry of the reaction given in eq 1 and the ^{18}O isotopic transfer reaction together show that during the catalytic reaction ATP is cleaved between the α-P atom and the αβ-bridge oxygen atom. By use of ATP containing different oxygen isotopes in the αβ-bridge and β-nonbridge positions

[e.g., ATP (**2a**)], the cleavage reaction shown in Scheme I leads to PP_i with different isotopes in the nonbridge positions of one phosphate group [PP_i (**4**)]. If the phosphate group with different oxygen isotopes rotates freely on the enzyme, then PIX might be observed in the absence of ammonia. The reisolated ATP would consist of a mixture of **2a** and **2b**, the relative ratios of which can be determined by ^{31}P NMR spectroscopy (Cohn & Hu, 1980; DeBrosse & Villafranca, 1983). By use of the PIX technique, the data in this paper provide the first kinetic evidence for the formation of an adenyl-XMP intermediate (**3**) in the reaction catalyzed by GMP synthetase.

EXPERIMENTAL PROCEDURES

Materials and Methods. GMP synthetase was isolated as a homogeneous preparation from *E. coli* B 96 (Crysler, 1984). Following the second DEAE-Sephadex column, the specific activity was 10 μmol min^{-1} mg^{-1} from the assay method of Moyed & Magasanik (1957). For routine assays, the method of Sakamoto (1978) was used, and the protein concentration was determined as described by Bradford (1976). $KH_2P^{18}O_4$ was prepared from $H_2^{18}O$ and PCl_5 (Risley & van Etten, 1978). All other chemicals were the highest purity available. Pyrophosphatase was a generous gift of Dr. Debra Dunnaway-Mariano of the University of Maryland.

Steady-State Kinetics. For most of the kinetic studies, the method of Moyed & Magasanik (1957) was used with the following modifications: the absorption drop at 290 nm due to the extinction difference ($\epsilon = 1.5 \times 10^3$ L mol^{-1} cm^{-1}) between XMP disappearance ($\epsilon = 4.8 \times 10^3$ L mol^{-1} cm^{-1}) and GMP appearance ($\epsilon = 3.3 \times 10^3$ L mol^{-1} cm^{-1}) was followed in 1.0-mL cuvettes. The pH was 8.5 and the temperature 39 °C unless otherwise noted. TAPS (160 mM) replaced Tris in the original assay, and the $MgCl_2$ concen-

---

[1] Abbreviations: PIX, positional isotope exchange; TAPS, 3-[[tris-(hydroxymethyl)methyl]amino]propanesulfonic acid.

Scheme I[a]
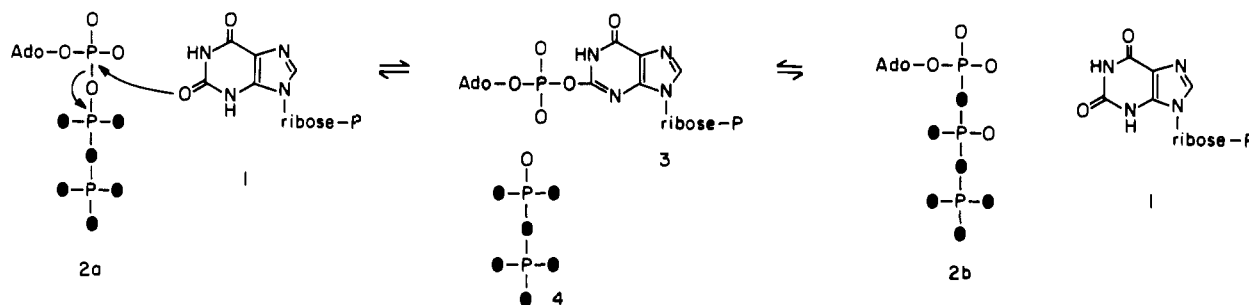
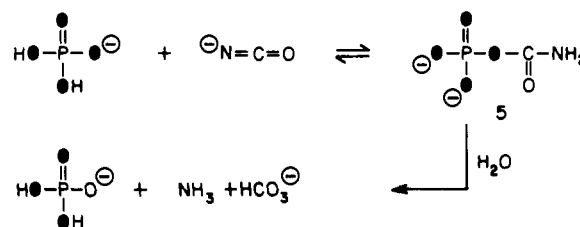[a] Solid oxygens designate [18]O.

Scheme II

Scheme III
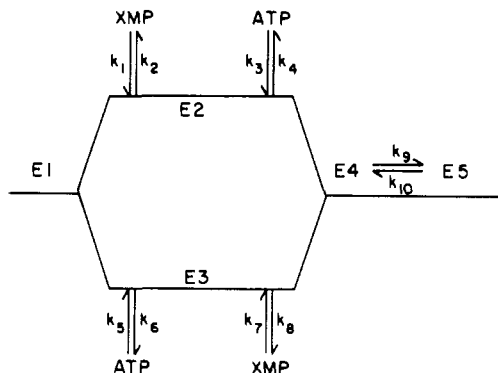
tration was adjusted to be at a 5-fold excess over the highest ATP concentration in all cases. The ionic strength was kept constant with KCl when ammonia salts were varied. For experiments where ATP was held constant, a coupled assay system using myokinase, pyruvate kinase, and lactate dehydrogenase was employed (Spector, 1978). Reaction conditions consisted of 10 units of salt-free myokinase, 20 units of pyruvate kinase, 25 units of lactate dehydrogenase, 1 mM phosphoenolpyruvate, 0.19 mM NADH, fixed levels of ATP, and 10 mM KCl in a 1.0-mL cuvette. The decrease in absorption at 339 nm was followed.

Kinetic data were fit to the Fortran programs of Cleland (1967) for intersecting or parallel patterns, and the σ value (square root of the average residual least square) was used as the criterion for the best fit. In no case did a set of data fit equally well to equations for both intersecting and parallel kinetic patterns.

Synthesis of $[\beta,\beta,\beta\gamma,\gamma,\gamma,\gamma\text{-}^{18}O_6]ATP$ (**2a**). Cohn & Hu (1980) had synthesized **2a** using coupled enzymatic reactions. Incubations of AMP, a trace of ATP, and carbamyl [[18]O$_4$]-phosphate (**5e** with myokinase and carbamate kinase resulted in a mixture of labeled AMP, ADP, and ATP **2a**. In our hands, this reaction was unsatisfactory, because the ATP **2a** was depleted of [18]O (97% [18]O in KH$_2$P[18]O$_4$ to 87% [18]O in **2a**). The reason for this is the instability of carbamyl phosphate, which is hydrolyzed partly by attack of water on the phosphorus atom (Allen & Jones, 1964). This leads to KH$_2$PO[18]O$_3$, which in turn reacts with KCNO to give depleted carbamyl phosphate (Scheme III). Therefore, some precautions were taken to avoid this and other complications. Carbamyl phosphate is formed by the second-order equilibrium reaction of cyanate anion (pK_a = 5.8) and phosphate anion (pK_a = 6.8) (Scheme III). Cyanic acid is unstable below pH 6.0 (Allen & Jones, 1964). The decomposition of carbamyl phosphate (half-life = 45 min at 37 °C between pH 1.5 and pH 8.5) with incorporation of [16]O into the resulting phosphate is faster at lower pH values, whereas C–O bond fission predominates above pH 6.5. Therefore, the synthesis of carbamyl phosphate was carried out between pH 6.5 and pH 7.5. An excess of cyanate over [[18]O$_4$]phosphate was used to drive the equilibrium to the side of the product. However, too high an excess of cyanate and long reaction times have to be avoided because its decomposition (half-life = 345 min at pH 6) results in the production of ammonia, which in turn attacks carbamyl phosphate (and cyanate) to form urea. This not only destroys the carbamyl phosphate, but the urea might later inactivate the coupling enzymes. The synthesis of carbamyl [[18]O$_4$]-phosphate and ATP **2a** were carried out as follows.

(*A*) *Carbamyl Phosphate Solution.* A total of 100 mg (694 μmol) of KH$_2$P[18]O$_4$ was added to a solution of 422 mg (5.21 mmol) of KCNO in 2.5 mL of water. After a 5-min incubation at 38 °C, 50 μL of glacial acetic acid was added and further incubated at 38 °C for 7 min.

(*B*) *Enzyme Solution.* In the meantime, 51.1 mg (140 μmol) of AMP (free acid, containing one H$_2$O) and 0.5 mg (0.8 μmol) of ATP (disodium salt, containing three H$_2$O) were dissolved in 5 mL of Tris buffer, pH 7.3. To this solution was added 75 μL of 1.0 M MgCl$_2$, 300 μL of 1.0 M KCl, 500 units of myokinase, and 50 units of carbamate kinase.

(*C*) *Reaction and Isolation.* The reaction was started by mixing the carbamyl phosphate solution and the enzyme solution and incubating at 38 °C. The reaction was followed by thin-layer chromatography (PEI–cellulose, 1.0 M LiCl). The R_f values were 0.6 (AMP), 0.4 (ADP), and 0.2 (ATP). After 30 min, the reaction was stopped by cooling (ice bath) and addition of 600 μL of 70% HClO$_4$. When the gas evolution ceased, the solution was filtered through glass wool. Then, a 2.0 M KOH solution was added to adjust the pH to 8.0, and KClO$_4$ was allowed to crystallize at 4 °C for 2 h. After filtration, the solution was applied to a 21 × 5 cm column of DEAE-cellulose (HCO$_3$$^-$ form) and washed with 100 mL of water. Elution was affected by a linear gradient of 4 L of triethylammonium bicarbonate buffer (0.035–0.35 M, pH 7.5). ATP was eluted at a concentration of 0.32 M. The solvent was removed at 40 °C and 20 Torr. The residue (tetraethylammonium salt of ATP **2a**) was then dissolved in 10 mL of methanol and stored at −20 °C. The yield was 77–83%, on the basis of the amount of AMP used. ATP **2a** contained 94 atom % [18]O.

Positional Isotope Exchange Experiments. GMP synthetase with a specific activity of 8 (units/mg) was incubated at
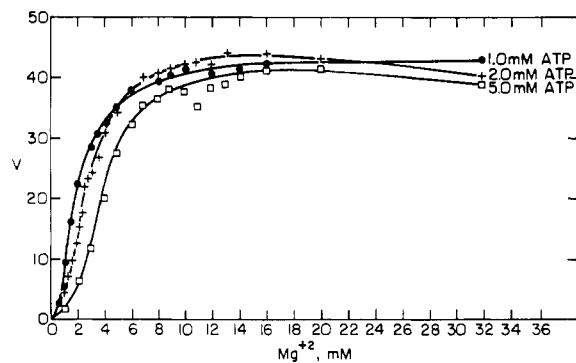
FIGURE 1: Velocity vs. [Mg^{2+}] at several ATP concentrations. Conditions: 160 mM Tris buffer, pH 8.5, 0.12 mM XMP, 200 mM NH$_4$Cl, 39 °C. The 290-nm continuous assay method was used to measure the enzyme velocity, which is given in arbitrary units. ATP concentrations are as indicated.
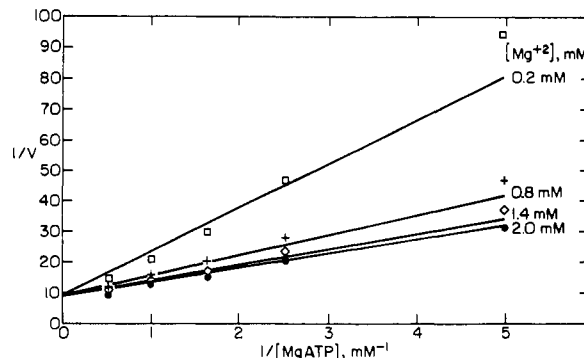

FIGURE 2: Double-reciprocal plot of velocity vs. [MgATP]. Conditions: 160 mM TAPS buffer, pH 8.5, 32 mM Gln, 0.2 mM XMP, 0.01 mM dithioerythritol. The 290-nm continuous assay method was used. The free Mg^{2+} concentrations are as given.

38 °C in 1-mL solutions (100 mM Tris buffer, pH 8.5) containing various levels of substrates for the PIX experiments. The reaction was stopped by the addition of 500 μL of a solution containing 0.2 M EDTA and 1.0 M Tris buffer, pH 8.5. Protein was removed by adding 4 drops of CCl$_4$, vortexing, and centrifuging. After the addition of 400 μL of [^{2}H$_6$]acetone, the solution was filtered through glass wool into a 10-mm NMR tube. The ^{31}P NMR spectrum was recorded at 145 MHz on a Bruker WM 360 spectrometer using a sweep width of 4200 Hz. A total of 1000 scans was accumulated with an acquisition time of 3.9 s. The couplings between the α-P atom and the protons of the ribose were removed by selective decoupling at about 4 ppm in the proton spectrum. With this method, only 0.1 of the energy of broad-band decoupling is necessary, which results in better resolution by avoiding heating of the sample.

Mathematical Model for the Partial Reaction. The method of net rate constants (Cleland, 1975) was applied to derive the kinetic expressions for the cases where either ATP or XMP binds first to the enzyme, followed by the other substrate. In Scheme II, E4 contains both substrates, and E5 contains the intermediate **3** and [^{18}O$_6$]PP$_i$ (**4**).

In the experimental protocols, the concentration of ATP is held constant while the XMP concentration is varied. For PIX to be observed, the reaction has to be reversible from the E5 complex until ATP is released from either E4 or E3 and $k_{10'}$ is the net rate constant that incorporates the PIX reaction and release of ATP from the enzyme:

$$V_{pix} = k_{10'}[E5] \tag{2}$$

From the kinetic expressions for the mechanism in Scheme II, two limiting cases can be presented. The first case is ordered addition of XMP before ATP (top branch of Scheme II):

$$V_{pix}/V_{cat} = k_6 k_9/(k_5 k_7 + k_7 k_9) \tag{3}$$

Equation 3 shows that V_{pix}/V_{cat} does not depend on the concentration of XMP. Therefore, the V_{pix} value is constant at any level of XMP. The second case is ordered addition of ATP before XMP (bottom branch of Scheme II):

$$V_{pix}/V_{cat} = k_2 k_4 k_6/\left\{k_7(k_2 k_4 + k_2 k_5 + k_3 k_5[XMP]) \times \left(1 + \frac{k_3 k_5 k_7[XMP]}{k_2(k_4 k_6 + k_4 k_7 + k_5 k_7)}\right)\right\} \tag{4}$$

Equation 4 shows that V_{pix}/V_{cat} depends on the XMP concentration at a constant ATP level. At both zero and satu-
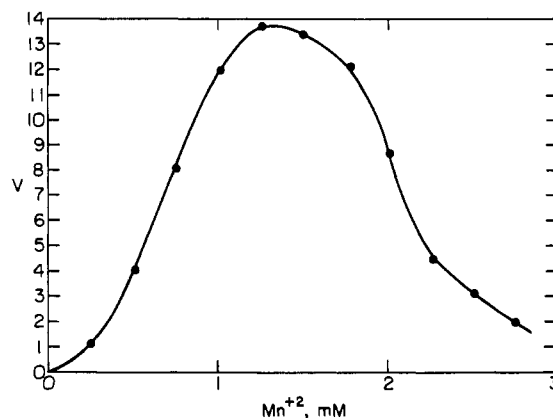
FIGURE 3: Velocity vs. [Mn^{2+}] at an ATP concentration of 2.0 mM. Conditions: 160 mM TAPS buffer, pH 8.5, 0.12 mM XMP, 200 mM NH$_4$Cl, 39 °C. The 290-nm continuous assay was used.

rating levels of XMP, the V_{pix}/V_{cat} is zero, and at some intermediate point this value reaches a maximum. Thus, the order of addition of substrates can be determined by the behavior of the PIX rate as the XMP concentration is varied.

RESULTS

Divalent Cation Requirements. The concentration of Mg^{2+} was varied at several fixed concentrations of ATP, and the effect on the reaction rate can be seen in Figure 1. Maximal activity is attained at Mg^{2+} concentrations 3–5-fold greater then the ATP concentration. This indicates the presence of additional metal ion binding sites other than the metal–ATP site. Thus, all assays were performed at Mg^{2+} concentrations (10 mM) 5-fold that of the highest concentration of ATP in order to occupy the metal–ATP and metal ion activating sites.

To estimate the dissociation constant of Mg^{2+} for the activating metal ion site, the reaction velocity vs. MgATP concentration was determined at various excess Mg^{2+} levels. The data in the double-reciprocal plot shown in Figure 2 were fit to the kinetic programs of Cleland (1967), and the dissociation constant for Mg^{2+} (0.7 ± 0.1 mM) at the metal ion activating site was determined. The pattern is that of equilibrium ordered (Cleland, 1970), with free Mg^{2+} binding before MgATP.

The effect of other divalent cations on the catalytic activity of GMP synthetase was also studied. Figure 3 shows the effect of Mn^{2+} on the reaction rate at an ATP concentration of 2.0 mM. Maximal activity was attained at a Mn^{2+} concentration approximately equal to half the ATP concentration, and additional Mn^{2+} was inhibitory. No activity was observed with Zn^{2+} or Co^{2+} as the divalent cation. The effect of Ca^{2+} is discussed later in this paper.

Table I: Initial Velocity Patterns

varied substrates	fixed substrate	pattern type	apparent Michaelis constant (mM)			
			MgATP	XMP	NH₄Cl	Gln
MgATP vs. XMP[a]	Gln, 46 mM	intersecting	0.22 ± 0.08	0.045 ± 0.012		
MgATP vs. XMP[a]	NH₄Cl, 200 mM	intersecting	0.32 ± 0.11	0.065 ± 0.024		
MgATP vs. NH₄Cl[a]	XMP, 0.2 mM	parallel	0.54 ± 0.03		41 ± 1	
MgATP vs. Gln[a]	XMP, 0.2 mM	parallel	0.24 ± 0.03			13 ± 1
XMP vs. NH₄Cl[b]	ATP, 10.5 mM	intersecting		0.319 ± 0.014	293 ± 15	

[a] The 290-nm continuous assay. [b] Myokinase, pyruvate kinase, and lactate dehydrogenase assay.

Initial Velocity Patterns. To establish the kinetic mechanism of GMP synthetase, the initial velocity patterns were determined for substrate pairs, and fit to the equations of Cleland as described under Experimental Procedures. The data are presented in Table I. MgATP vs. XMP with either ammonia or glutamine gave intersecting patterns while MgATP vs. either NH₄Cl or glutamine, at a fixed concentration of XMP, resulted in parallel patterns. XMP vs. NH₄Cl gave an intersecting pattern. The XMP vs. glutamine pattern could not be determined by the 290-nm continuous assay due to the limitations of the assay, and other assay methods with coupled enzyme systems were not suitable (Crysler, 1984). At levels of XMP near the K_m value ($\sim$0.04 mM), the MgATP vs. NH₄Cl patterns were intersecting, but extensive data were not obtained due to limitations with the assay procedures.

Synthesis of ATP 2a. A new method (see Experimental Procedures) was developed to improve the yield of carbamyl [¹⁸O₄]phosphate. This method yields 70% carbamyl [¹⁸O₄]-phosphate (based on the amount of KH₂P¹⁸O₄) in 10 min. ATP 2a was then synthesized from carbamyl [¹⁸O₄]phosphate. The pH of the solutions was adjusted and maintained at 7.3-8.0 because, above this pH, the decomposition of carbamyl phosphate becomes very fast. Following this procedure, the synthesis of ATP 2a takes only about 30 min. After column chromatography, the yield is 77-83%, and the ¹⁸O content is 94 atom %.

Catalytic Reactions. When GMP synthetase was incubated with ATP 2a, the enzyme catalyzes the production of [¹⁸O₆]PPᵢ (4) and AMP only in the presence of Mg²⁺ and XMP. PPᵢ (4) was identified by its ³¹P NMR spectrum (Figure 4). The two phosphate groups in unsymmetrically ¹⁸O-substituted pyrophosphates like 4 are not equivalent. Therefore, one observes an AB spin system[2] in the ³¹P NMR spectrum of 4. The experimentally determined chemical shifts and concentrations of the various possible ¹⁸O-substituted PPᵢ species were as expected (Table II).

As shown in Table III, the rate of PPᵢ production depends on the concentration of XMP. No PPᵢ production was observed in the absence of XMP. In the presence of 1 mM XMP, the rate was constant over a period of 160 min (Table III).

PIX Experiments. GMP synthetase catalyzes the exchange of ¹⁸O from the β-nonbridge positions of [β,β,βγ,γ,γ,γ-

[2] For unsymmetrically ¹⁸O-substituted PPᵢ at 145.81 MHz, the ³¹P-³¹P coupling constant is much larger (21.1 Hz) (Marschner et al., 1983; Lowe & Potter, 1984) than the chemical shift difference between the phosphate groups. Therefore, only the inner lines of the AB spin system can be observed as an unresolved singlet, the chemical shift of which is at the center between the individual shifts of the phosphate groups. The ¹⁸O isotope induced chemical shift per ¹⁸O bonded is 0.0219 ppm (Marschner et al., 1983). With this value, one calculates the chemical shift of [¹⁸O₆]PPᵢ (4) to be 0.0766 ppm upfield from unlabeled PPᵢ. The peak at highest field in Figure 1 (0.0767 ppm upfield from PPᵢ) was therefore assigned to 4. The signals on the low-field side of the peak result from PPᵢ containing less ¹⁸O than 4. This is due to incompletely labeled ATP 2a and not to washout of ¹⁸O during the enzymatic reaction. Two batches of ATP 2a containing 94% and 89% ¹⁸O, respectively, were used to confirm this result.
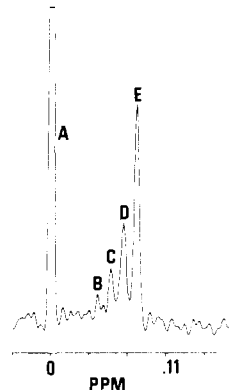

FIGURE 4: ³¹P NMR spectrum of PPᵢ produced by the reaction of GMP synthetase with ATP 2a. The reaction conditions are given under Experimental Procedures. The peak marked A is [¹⁶O₇]PPᵢ and the peaks marked B–E are for the PPᵢ species identified in Table II.
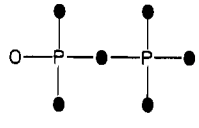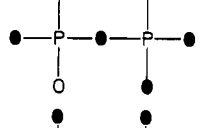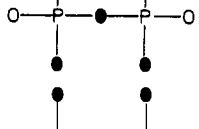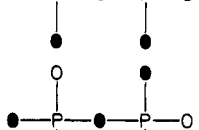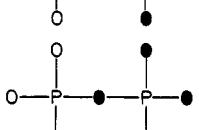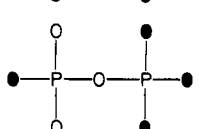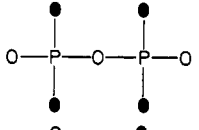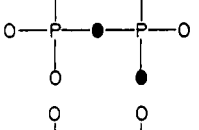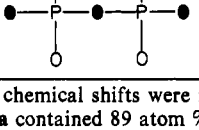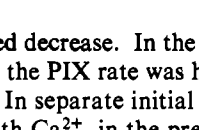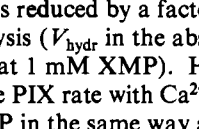
¹⁸O₆]ATP (2a) into the αβ-bridge position only in the presence of XMP and Mg²⁺. The PIX rate was constant over a period of 160 min in the presence of 1 mM XMP (Table III). The data also show that the γ-phosphate group of ATP 2a was depleted of ¹⁸O during the reaction. This is evidence that [¹⁸O₆]PPᵢ (4) also attacks intermediate 3 with the fully ¹⁸O-labeled phosphate group that originated from the γ-P of ATP 2a. For entry four in Table III, at 120 min and 13% ATP hydrolyzed, the 0.33 scrambling reached was due to ~30% from the dissociation/reassociation of PPᵢ on the basis of the percent of ¹⁸O depleted in the γ-P of ATP and the remainder from PIX of the β-P of bound PPᵢ. Smith & Cohn (1981) demonstrated that Val- and Met-tRNA synthetases interchange the β- and γ-phosphoryl groups of ATP without release of PPᵢ into solution so this reaction has precedent.

To test the possibility that the [¹⁸O₆]PPᵢ (4) free in solution (produced by the catalytic hydrolysis) can rebind to the enzyme complex still containing intermediate3, two experiments were conducted: removal of all free PPᵢ (by enzymatic reaction) or addition of an excess of unlabeled PPᵢ (ATP/PPᵢ exchange experiment). To remove PPᵢ, pyrophosphatase was added to the incubation mixtures, and this resulted in a decreased PIX rate (Table III). The PIX rate could not be brought to zero, however. Incubation with a higher concentration of pyrophosphatase was not possible, because this enzyme also acts as an ATPase (Gonzalez et al., 1984). When unlabeled pyrophosphate was added to an incubation mixture, no PIX was detected. However, unlabeled ATP was produced. In Table IV data are presented that show that the production of unlabeled ATP (ATP/PPᵢ exchange) depended on the XMP concentration.

PIX Experiments in the Presence of Ca²⁺ Ions. The previous experiments indicated that GMP synthetase catalyzes ATP/PPᵢ exchange. To remove the PPᵢ produced by the catalytic hydrolysis, we added CaCl₂ because the calcium salt of PPᵢ is insoluble at pH 8.5. The data in Table V show that the PIX rate (V_{pix}/V_{cat}) remained constant instead of the

Table II: Calculated and Experimental Chemical Shifts and Distribution of Various ^{18}O-Labeled Pyrophosphates Obtained by Incubating ATP 2a with GMP Synthetase[a]

compd	chemical shift		peak in Figure 1	fraction[b]		fraction[c]	
	calcd	found		calcd	found	calcd	found
(structure)	0.0766	0.0767	E	0.69	0.68	0.50	0.50
(structure)	0.0657	0.0653	D	0.09		0.12	
(structure)					0.24		0.28
(structure)				0.13		0.18	
(structure)	0.0547	0.0540	C	0.04		0.06	
(structure)				0.02	0.06	0.05	0.15
(structure)				0.005		0.01	
(structure)	0.0438	0.0425	B	0.005		0.02	
(structure)				0.01		0.02	
(structure)					0.02		0.07
(structure)							0.005

[a]The chemical shifts were relative to PP_i and were calculated from the value of Marschner et al. (1983). [b]ATP 2a contained 94 atom % [18]O. [c]ATP 2a contained 89 atom % [18]O (Figure 4).

expected decrease. In the presence of Ca^{2+} alone (absence of Mg^{2+}), the PIX rate was higher than in the presence of Mg^{2+} alone. In separate initial velocity experiments, the catalytic rate with Ca^{2+}, in the presence of NH_3, was measured, and V_{cat} was reduced by a factor of $1/_{59}$ while the rate of catalytic hydrolysis (V_{hydr} in the absence of NH_3) was not measurable at all (at 1 mM XMP). However, the data in Table V show that the PIX rate with Ca^{2+} still depends on the concentrations of XMP in the same way as in the presence of Mg^{2+} peaking at $\sim$0.5–1.0 mM XMP and then dropping at high concentrations of XMP.

PIX Experiments in the Presence of Psicofuranine. Psicofuranine is known to act as an irreversible inhibitor of GMP synthetase (Spector & Beacham, 1975). In our experiments,

we found that the rate of catalytic hydrolysis is indeed reduced to zero if the enzyme is preincubated for 20 min at 38 °C in the presence of XMP, PP_i, Mg^{2+}, and psicofuranine. However, the data presented in Table VI show that neither the PIX rate nor the ATP/PP_i exchange rate are affected by the presence of psicofuranine.

DISCUSSION

From the data presented in this paper, it is clear that GMP synthetase requires free Mg^{2+} in addition to MgATP for catalysis. At least a 3-fold Mg^{2+} excess over the ATP concentration is required for full activity (Figure 1). The initial velocity pattern of $[Mg^{2+}]_{free}$ vs. [MgATP] (Figure 2) is of the equilibrium-ordered[b] type, indicating that free Mg^{2+} pro-

Table III: PIX Experiments in the Presence of Mg^{2+} [c]

enzyme (µg)	ATP (mM)	XMP (mM)	MgCl₂ (mM)	min	fraction of ATP hydrolyzed	fraction of scrambling equilibrium reached	V_{hydr}/V_{cat}	V_{pix}/V_{cat}
0	1.0	1.0	5.0	120	0	0		
180	1.0	0	5.0	120	0	0		
180	1.0	1.0	0	120	0	0		
180	1.0	1.0	5.0	120	0.13	0.33	0.0009	0.002
330	1.7	1.0	5.0	10	0	0.05		0.002
				20	0.02	0.11	0.0006	0.002
				40	0.05	0.17	0.0008	0.002
				80	0.09	0.29	0.0007	0.002
				160	0.20	0.53	0.0008	0.002
180	1.0	0.02	5.0	120	0.04	0.14	0.0002	0.0009
		0.1			0.11	0.32	0.0006	0.0021
		0.5			0.14	0.33	0.0008	0.0022
		1.0			0.13	0.37	0.0008	0.0025
		2.0			0.16	0.40	0.0009	0.0027
		4.0			0.25	0.34	0.0015	0.0021
		8.0			0.32	0.31	0.0019	0.0018
270	1.0	1.0	10.0	90	0.22	0.25	0.0012	0.002
270[b]					0.40	0.20	0.0020	0.001

[a] The reaction conditions are given under Experimental Procedures. To calculate the final scrambling equilibrium value for the $\alpha\beta$-bridge position, a ratio of 1:5 ^{16}O:^{18}O was used due to the dissociation/reassociation of PP_i (see text). [b] In this experiment, 5 units of pyrophosphates was added. No PP_i signal was observed. The rate of hydrolysis was determined by the NMR signals due to P_i.

Table IV: ATP/PP$_i$ Exchange Experiments[a]

XPM (mM)	fraction of exchange equilibrium reached	V_{exch}/V_{cat}
0	0	0
0.1	29	0.0015
0.5	59	0.0035
1.0	61	0.0035
2.0	57	0.0030
6.0	47	0.0025
30.0	0	0

[a] Reaction conditions: 1-mL solutions containing 1.0 mM ATP **2a** 1.0 mM PP_i, 10.0 mM $MgCl_2$, 270 µg of GMP synthetase, and various amounts of XMP in 100 mM Tris, pH 8.5, were incubated at 38 °C for 120 min.

ceeds MgATP binding. The presence of a divalent metal ion activating site other than the MgATP site has been shown for other enzymes, including PEP carboxykinase (Foster et al., 1967), glutamine synthetase (Hunt et al., 1975), pyruvate kinase (Gupta et al., 1976), and carbamoyl-phosphate synthetase (Raushel et al., 1978). An equilibrium-ordered pattern for $[Mg^{2+}]_{free}$ vs. [MgATP] was demonstrated for carbamoyl-phosphate synthetase derived from both *E. coli* (Raushel et al., 1979) and bovine liver (Elliot & Tipton, 1974).

With Mn^{2+} as the divalent metal, maximal activity was achieved at a Mn^{2+} concentration of approximately half the ATP concentration (Figure 3). Mn^{2+} concentrations greater than 50% of the ATP concentration are inhibitory. These data suggest that Mn^{2+} binds to the MnATP catalytic site, the

divalent metal ion activating site, and an inhibitory site. This phenomenon has also been observed with *E. coli* carbamoyl-phosphate synthetase (Raushel et al., 1979).

The initial velocity kinetic data presented in this paper along with the preliminary studies of Fukuyama (1966) and Spector & Beacham (1975) are consistent with the order of addition of substrates in the bottom branch of Scheme II. Using the rules of Cleland (1963), the rationale for this kinetic mechanism is as follows: (1) The MgATP vs. XMP pattern is intersecting, indicating that MgATP and XMP bind without intervening product release or amide binding. (2) No addition or release separates XMP and NH_4Cl binding due to the intersecting XMP vs. NH_4Cl pattern. The parallel pattern of MgATP vs. either NH_4Cl or glutamine at saturating XMP shows that XMP must bind between MgATP and the ammonia source. (3) MgATP and XMP can bind in the absence of ammonia or glutamine. These data are consistent with the formation of the adenyl-XMP intermediate (3) described by Fukuyama (1966). This suggests either an ordered addition where ammonia (or glutamine) binds after MgATP and XMP (bottom branch of Scheme IV), or a partially random addition where ammonia can bind before or after MgATP/XMP (top branch of Scheme IV). (4) The determination by Spector & Beacham (1975) that pyrophosphate is a competitive inhibitor vs. ATP, and therefore binds to the same enzyme form (Cleland, 1963), suggests that pyrophosphate is the last product released. The top branch of Scheme IV is therefore

Table V: PIX Experiments in the Presence of Ca^{2+} [a]

| XMP (mM)	MgCl₂ (mM)	CaCl₂ (mM)	fraction of ATP hydrolyzed	fraction of scrambling equilibrium	V_{hydr}/V_{cat}	V_{pix}/V_{cat}
1.0	10		0.21	0.27	0.0011	0.0014
	10	10	0.16	0.24	0.0008	0.0015
		10	0	0.49	0	0.0035
0		10	0	0	0	0
0.1			0	0.52	0	0.0038
0.5			0	0.58	0	0.0047
2.0			0	0.58	0	0.0047
5.0			0	0.51	0	0.0037
10.0			0.08	0.43	0.0006	0.0028
30.0			0.11	0.39	0.0008	0.0024

[a] Reaction conditions: 1-mL solutions of 1.0 mM ATP **2a** and 270 µg of GMP synthetase were incubated at 38 °C for 90 min. V_{cat} is the catalytic rate under standard conditions (Sakamoto, 1978).

Table VI: PIX and ATP/PP$_i$ Exchange Experiments in the Presence of Psicofuranine[a]

PP$_i$ (mM)	psicofuranine (mM)	fraction of ATP hydrolyzed	fraction of exchange or scrambling equilibrium reached	V_{hydr}/V_{cat}	V_{pix}/V_{cat}
0.1	0	0.05	0.29	0.0007	0.0026
0.1	0.2	0	0.25	0	0.0022
1.0	0	0.13	0.28	0.0010	0.0020
1.0	0.2	0	0.29	0	0.0022

[a] Conditions: 1-mL solutions containing 10.0 mM MgCl$_2$, 2.0 mM XMP, 270 μg of GMP synthetase, and PP$_i$ and psicofuranine as indicated in 100 mM Tris buffer, pH 8.5, were incubated at 38 °C for 20 min. The reactions were started by the addition of ATP **2a** (1.0 mM) and then incubated for an additional 60 min.

Scheme IV
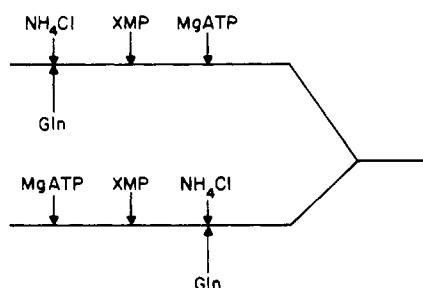
eliminated as pyrophosphate would be noncompetitive vs. ATP or uncompetitive at saturating substrate concentrations.

The proposed mechanism of addition presented here differs from that of Zyk et al. (1969), who propose an ordered addition of XMP and ATP, respectively. Their mechanism is based on the observation that XMP alone, or XMP in combination with ATP, results in a protection of GMP synthetase from inactivation by heat or proteolysis. Since ATP alone did not afford any protection from inactivation, the authors proposed that XMP must bind first in order to allow subsequent ATP binding.

Other possibilities that could explain the apparent substrate binding observed by Zyk et al. (1969) include nonspecific binding under these conditions, binding to the proteolytic enzymes with subsequent inhibition, and binding to altered conformations of GMP synthetase due to heat treatment or limited proteolytic digestion.

Additional support for the kinetic mechanism of GMP synthetase (bottom branch of Schemes II and IV), which involves ordered addition of substrates with MgATP binding first followed by XMP, derives from the PIX experiments. These data showed a rise followed by a decline of both the PIX rate and the ATP/PP$_i$ exchange rate as the XMP concentration was increased. The decrease occurs because ATP is not released from the enzyme as predicted from the kinetic mechanism and the ATP is trapped in the E4 complex (Scheme II). The possibility that XMP behaves as a simple inhibitor vs. ATP is eliminated because both the hydrolysis and the catalytic rate are not lowered at high XMP concentrations.

The hydrolysis of ATP to AMP and PP$_i$ catalyzed by GMP synthetase was reported earlier (Fukuyama, 1966). Presumably, water attacks intermediate 3 in the same way as ammonia does in the normal catalytic reaction, but the possibility that the intermediate dissociates from the enzyme and is then hydrolyzed nonenzymatically cannot be ruled out.

When Ca^{2+} is substituted for Mg^{2+}, the rates of hydrolysis and the catalytic reaction are reduced considerably. This means that some step in the forward reaction catalyzed by GMP synthetase is decreased. However, the PIX rate is increased in the presence of Ca^{2+}, and therefore, intermediate 3 is produced faster than the subsequent attack of water or ammonia. Several possible explanations for this result can be considered. The observation of PIX depends on two steps that are not normal components of the enzymatic reaction under initial velocity conditions: (1) establishment of torsional symmetry of one phosphate group of PP$_i$ (4) and (2) release of ATP by reversal of the catalytic reaction. One of these steps could be rate limiting for the scrambling reaction (Rose, 1979). Nothing is known about the rate of dissociation of the Mg–O–P bond relative to Ca–O–P when bound to the enzyme, and this could be important in determining the rate of rotation of bound PP$_i$ in the PIX reaction. Another possibility is that MgPP$_i$ might dissociate faster than CaPP$_i$ from the E5 enzyme complex, leading to rapid reaction of NH$_3$ (V_{cat}) or H$_2$O (V_{hydr}) with the adenyl-XMP intermediate (3). If MgATP release is slower than CaATP release, then this would also contribute to the increased PIX and exchange rates observed in the presence of Ca^{2+}. As PP$_i$ is also an inhibitor vs. ATP (Spector & Beacham, 1975), the high concentration of PP$_i$ in the exchange reaction should lead to competion with the ATP and thus lower the forward reaction, whereas it should also increases the back-reaction. The result might be the constant PIX rate observed with varying PP$_i$ concentrations (Table V). All of these considerations are reasonable explanations of the observed data when one remembers that the PIX rate depends on the relative rates of k_9/k_{10} and the release of product from E5 relative to ATP (Mg^{2+} or Ca^{2+}) release.

Finally, we observed that the PIX and exchange rates are not affected when the enzyme is inhibited with psicofuranine. From these experiments, we conclude that the formation of intermediate 3 is not inhibited by the presence of psicofuranine in constrast to an earlier report (Fukuyama, 1966). With the fact that psicofuranine does not change the binding constants of ATP and XMP (Udaka & Moyed, 1963), the mode of inhibition by this compound seems to result from interference with only with the second part of the reaction, namely, the attack of nucleophiles on intermediate 3.

REFERENCES

Abrams, R., & Bentley, M. (1959) *Arch. Biochem. Biophys.* 79, 91–110.
Allen, C. M., & Jones, M. E. (1964) *Biochemistry 3*, 1238–1247.
Bradford, M. M. (1976) *Anal. Biochem. 72*, 248–254.
Cleland, W. W. (1963) *Biochim. Biophys. Acta 67*, 104–137.
Cleland, W. W. (1967) *Adv. Enzymol. Relat. Areas Mol. Biol.* 29, 1–32.
Cleland, W. W. (1970) *Enzymes (3rd Ed.)* 2, 1–65.
Cleland, W. W. (1975) *Biochemistry 14*, 3220–3224.
Cohn, M., & Hu, A. (1980) *J. Am. Chem. Soc. 102*, 913–916.
Crysler, C. (1984) M.S. Thesis, The Pennsylvania State University.
DeBrosse, C. W., & Villafranca, J. J. (1983) in *Magnetic Resonance in Biology* (Cohen, S., Ed.) pp 1–52, Wiley, New York.
Elliot, K. R. F., & Tipton, K. F. (1974) *Biochem. J. 141*, 807–816.
Foster, D. O., Lardy, H. A., Ray, P. D., & Johnston, J. B. (1967) *Biochemistry 6*, 2120–2128.
Fukuyama, T. T. (1966) *J. Biol. Chem. 241*, 4745–4749.
Gonzales, M. A., Webb, M. A., Welsh, K. M., & Cooperman, B. S. (1984) *Biochemistry 23*, 797–801.
Gupta, R. K., Fung, C. H., & Mildvan, A. S. (1976) *J. Biol. Chem. 251*, 2421–2430.

Hunt, J. B., Smyrniotis, P. Z., Ginsburg, A., & Stadtman, E. R. (1975) *Arch. Biochem. Biophys. 166,* 102–124.

Lagerkvist, U. (1956) *J. Biol. Chem. 233,* 143–149.

Lowe, G., & Potter, B. V. L. (1984) *J. Chem. Soc., Chem. Commun.,* 877–879.

Marschner, T. M., Reynolds, M. A., Oppenheimer, N. J., & Kenyon, G. L. (1983) *J. Chem. Soc., Chem. Commun.,* 1289–1290.

Midelfort, C. F., & Rose, I. A. (1976) *J. Biol. Chem. 251,* 5881–5887.

Moyed, H. S., & Magasanik, B. (1957) *J. Biol. Chem. 226,* 351–363.

Raushel, F. M., & Garrard, L. J. (1984) *Biochemistry 23,* 1791–1795.

Raushel, F. M., Anderson, P. M., & Villafranca, J. J. (1978) *Biochemistry 17,* 5587–5591.

Raushel, F. M., Rawding, C. J., Anderson, P. M., & Villafranca, J. J. (1979) *Biochemistry 18,* 5562–5566.

Risley, J. M., & van Etten, R. L. (1978) *J. Labelled Compd. Radiopharm. 15,* 533–537.

Rose, I. A. (1979) *Adv. Enzymol. Relat. Areas Mol. Biol. 50,* 361–395.

Sakamoto, N. (1978) *Methods Enzymol. 51,* 213–218.

Smith, L. T., & Cohn, M. (1981) *Biochemistry 20,* 385–391.

Spector, T. (1978) *Methods Enzymol. 51,* 219–224.

Spector, T., & Beacham, L. M. (1975) *J. Biol. Chem. 250,* 3101–3107.

Udaka, S., & Moyed, H. S. (1963) *J. Biol. Chem. 238,* 2797–2803.

Zyk, N., Citri, N., & Moyed, H. S. (1969) *Biochemistry 8,* 2787–2794.

Spectral and Kinetic Studies of Metal-Substituted *Aeromonas* Aminopeptidase: Nonidentical, Interacting Metal-Binding Sites[†]

John M. Prescott*

Institute of Occupational Medicine, College of Medicine, Texas A&M University, College Station, Texas 77843

Fred W. Wagner

Department of Agricultural Biochemistry, University of Nebraska, Lincoln, Nebraska 68583

Barton Holmquist and Bert L. Vallee

Center for Biochemical and Biophysical Sciences and Medicine, Harvard Medical School, Boston, Massachusetts 02115

Received March 12, 1985

ABSTRACT: Apoenzyme prepared by removal of the 2 mol of Zn^{2+}/mol from *Aeromonas* aminopeptidase is inactive. Addition of Zn^{2+} reactivates it completely, and reconstitution with Co^{2+}, Ni^{2+}, or Cu^{2+} results in a 5.0-, 9.8-, and 10-fold more active enzyme than native aminopeptidase, respectively. Equilibrium dialysis and spectral titration experiments with Co^{2+} confirm the stoichiometry of 2 mol of metal/mol. The addition of only 1 mol of metal/mol completely restores activity characteristic of the particular metal. Interaction between the two sites, however, causes hyperactivation; thus, addition of 1 mol of Zn^{2+}/mol subsequent to 1 mol of Co^{2+}, Ni^{2+}, or Cu^{2+} per mole increases activity 3.2-, 42-, or 59-fold, respectively. The cobalt absorption spectrum has a peak at 527 nm with a molar absorptivity of 53 M^{-1} cm^{-1} for 1 mol of cobalt/mol, which increases to 82 M^{-1} cm^{-1} for a second cobalt atom and is unchanged by further addition of Co^{2+}. Circular dichroic (CD) and magnetic CD spectra indicate that the first Co^{2+} binding site is tetrahedral-like and that the second is octahedral-like. Stoichiometric quantities of 1-butylboronic acid, a transition-state analogue inhibitor of the enzyme [Baker, J. O., & Prescott, J. M. (1983) *Biochemistry 22,* 5322], profoundly affects absorption, CD, and MCD spectra, but *n*-valeramide, a substrate analogue inhibitor, has no effect. These findings suggest that the tetrahedral-like site is catalytic and the other octahedral-like site is regulatory or structural.

Aeromonas aminopeptidase, isolated from culture filtrates of *Aeromonas proteolytica*, is a zinc metalloenzyme (Prescott & Wilkes, 1966) and contains 2 mol of zinc/mol (Prescott et al., 1971). The apoenzyme is inactive, but reconstitution with Zn^{2+} restores full activity, and its substitution by Co^{2+}, Ni^{2+}, or Cu^{2+} substantially increases activity over that of the native enzyme. Moreover, the addition of 1 mol of Zn^{2+}/mol to aminopeptidase reconstituted with 1 mol of either Cu^{2+} or Ni^{2+} per mole results in hyperactivation of *Aeromonas* aminopeptidase (Prescott et al., 1983). We have now examined the kinetics and spectral consequences of metal ion substitutions at the active site of cobalt *Aeromonas* aminopeptidase, using cobalt as a chromophoric probe, to monitor the interaction of the two metal binding sites with different metal permutations.

EXPERIMENTAL PROCEDURES

Materials. Tricine[1] and Hepes were obtained from both